Quantum Plasmonic Circuits

Nathalie P. de Leon, Mikhail D. Lukin, and Hongkun Park

(Invited Paper)

***Abstract*—Interactions between light and matter can be dramatically modified by concentrating light into a small volume for a long period of time. Gaining control over such interaction is critical for realizing many schemes for classical and quantum information processing, including optical and quantum computing, quantum cryptography, and metrology and sensing. Plasmonic structures are capable of confining light to nanometer scales far below the diffraction limit, thereby providing a promising route for strong coupling between light and matter, as well as miniaturization of photonic circuits. At the same time, however, the performance of plasmonic circuits is limited by losses and poor collection efficiency, presenting unique challenges that need to be overcome for quantum plasmonic circuits to become a reality. In this paper, we survey recent progress in controlling emission from quantum emitters using plasmonic structures, as well as efforts to engineer surface plasmon propagation and design plasmonic circuits using these elements.**

***Index Terms*—Integrated photonic circuits, optoelectronic devices, plasmons, quantum optics.**

I. Introduction

THE absorption probability of a single photon by a single atom is typically very weak because there is a large mismatch between the optical absorption cross section of an atomic transition and the diameter of the excitation beam. Similarly, efficient collection of single photons is difficult due to the mismatch between a dipole emission pattern and an optical mode. The interaction between a single photon and a single emitter can be enhanced using several strategies. For a radiatively broadened transition, the absorption cross section of a quantum emitter is proportional to the absorption wavelength squared (λ^2) [1], and efficient absorption can be achieved by tightly focusing the incident beam [2]–[4]. Unfortunately, this technique is not effective for transitions broadened due to dephasing, as is typically the case in solid-state emitters. Another strategy is to place the emitter into a high finesse macroscopic or nanophotonic cavity, giving the photon many chances to interact with it [5]. Finally, an emitter can be placed next to a plasmonic structure where the electromagnetic excitation can be arbitrarily confined well below the diffraction limit [6], [7]. In such a configuration, light can be concentrated to match the small absorption cross section of the emitter and slowed due to a reduced group velocity to further enhance the photon-emitter coupling. This phenomenon is the basis of quantum plasmonics.

When light impinges on a metal–dielectric interface, it can induce charge density oscillations bound to the electromagnetic field oscillation. This phenomenon has been theoretically understood for over a century: the extinction properties of small metallic particles were first described by Mie in 1908 [8], and plasma oscillations in thin metallic films were quantitatively described by Ritchie in 1957 [9]. Recent developments in micro- and nanofabrication and synthesis have led to renewed efforts in the field of plasmonics [10]–[14]. In metallic particles smaller than the wavelength of light, the confinement of conduction electrons provides a restoring force that leads to a peak in extinction known as a localized surface plasmon (LSP) resonance. Numerous research efforts over the past decades have focused on characterizing and manipulating LSPs of small particles, leading to exquisite control over particle shape and size, generating rods [15], [16], shells [17], [18], rings [19], platonic solids [20]–[22], and heterostructures [23]. LSPs have also been exploited for plasmonic antennas [24], gratings [10], [12], and hole arrays exhibiting extraordinary transmission [25], [26]. There have also been several studies showing control over the plasmon resonance via interparticle interaction [27] and plasmon mode hybridization [28], [29]. Together, these techniques can be used to tune LSPs over the entire visible range into the near IR. The traditional applications of this work have been in sensing and for use as surface-enhanced Raman spectroscopy substrates [30], [31]. Many studies have also demonstrated the use of these plasmonic nanoparticles in enhancing absorption and scattering in photovoltaics [32], photoelectrochemical cells [33], [34], and other energy-harvesting devices. Recently, sophisticated multinanoparticle structures have been shown to display interesting effects, such as quantum interference between different plasmonic decay channels [35].

In metallic films, charge oscillations can propagate along the metal–dielectric interface at frequencies below the material plasmon resonance. These propagating surface plasmon polaritons (SPPs) are distinct from LSPs in that they have a nonzero real component of their wave vector, i.e., they have a well-defined propagation direction. SPPs can be waveguided and manipulated like photons, thereby opening up the prospect of designing integrated plasmonic devices and circuits, analogous to integrated photonics and electrical circuits [10], [14]. These plasmonic circuits can confine and guide light well below the diffraction

Manuscript received February 27, 2012; revised April 23, 2012; accepted April 24, 2012. This work was supported in part by the National Science Foundation (NSF), Defense Advanced Research Projects Agency, the Packard Foundation, and the NSF and National Defense Science and Engineering Graduate Research Fellowships.

N. P. de Leon and H. Park are with the Departments of Physics and Chemistry and Chemical Biology, Harvard University, Cambridge, MA 02138 USA (e-mail: deleon@fas.harvard.edu; hongkun_park@harvard.edu).

M. D. Lukin is with the Department of Physics, Harvard University, Cambridge, MA 02138 USA (e-mail: lukin@physics.harvard.edu).

Color versions of one or more of the figures in this paper are available online at http://ieeexplore.ieee.org.

Digital Object Identifier 10.1109/JSTQE.2012.2197179

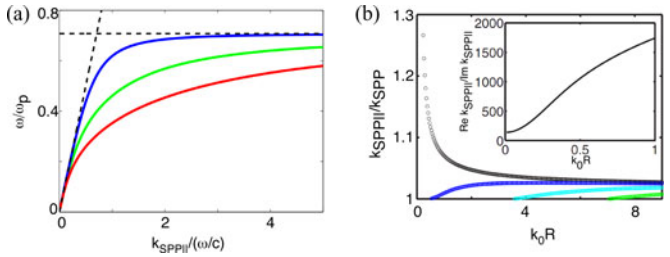

Fig. 1. (a) Dispersion relationship for a flat metal–dielectric interface (blue) and the fundamental modes of a 1-D plasmonic waveguide of radius $R = 0.5/k_0$ (green) and $R = 0.2/k_0$ (red). (Reproduced with permission from [36]) (b) Allowed modes $k_{\mathrm{SPP}||}$ as a function of R, where k_{SPP} is the wave vector in the metal medium. Higher order modes show cutoff, while the fundamental mode (black) exhibits a $k_{\mathrm{SPP}||} \propto 1/R$ dependence. Inset shows the propagation length for the fundamental mode as a function of R (Reproduced with permission from [7]). For both figures, the metal is silver, and the surrounding dielectric has dielectric constant $= 2$.

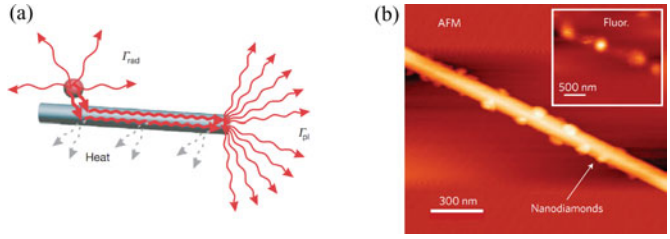

Fig. 2. Coupling to quantum emitters. (a) Schematic of quantum dot emission into SPPs in a nanowire waveguide (reproduced with permission from [45]). The quantum dot can radiate into the far field (Γ_{rad}) or into SPPs, where they can nonradiatively decay as heat, or scatter back into the far field at the end of the nanowire (Γ_{p1}). (b) AFM image of nanodiamonds decorating a silver nanowire (reproduced with permission from [49]). Inset shows fluorescence from NVs in the nanodiamonds.

limit, and thus have natural applications toward sensing, optoelectronic interfacing, and Purcell enhancement of emission.

Compared with a free-space photon of the same frequency, an SPP has higher momentum, lower group velocity, and greater spatial confinement. The SPP is characterized by its wave vector k_{SPP}: $k_{\mathrm{SPP}} = k_0\sqrt{\frac{\varepsilon_d\varepsilon_m}{\varepsilon_d+\varepsilon_m}}$ where k_0 is the free-space wave vector, ε_m is the dielectric constant of the metal, and ε_d is the dielectric constant of the surrounding dielectric medium. The dispersion relationship for SPPs (see Fig. 1) bends away from the light line ($k_{\mathrm{SPP}} > k_0$) and k_{SPP} goes to infinity as the frequency asymptotically approaches the material plasmon resonance ($\omega = \omega_{\mathrm{SP}}/\sqrt{2}$): consequently, the momentum of the SPP becomes very large, the wavelength becomes small, and the effective impedance approaches infinity near the plasmon resonance. This dispersion enables the confinement of light to deep subwavelength dimensions close to the plasmon resonance.

Special plasmonic waveguide geometries enable the confinement of light to arbitrarily small, subwavelength dimensions away from the plasmon resonance [36]–[38]. For example, in a cylindrical plasmonic waveguide, the electric field intensity is bound to the surface even for arbitrarily small radii. This is in stark contrast to a dielectric waveguide (such as an optical fiber), for which as the radius shrinks below the diffraction limit, the first-order guided mode becomes exponentially unconfined. The existence of a bound, confined, fundamental mode as the radius approaches zero is unique to plasmonic waveguides, but not restricted to the cylindrical, 1-D geometry. Over recent years, a variety of waveguide geometries, including arrays of metallic dots [39], metal–insulator–metal (MIM) structures [40], metallic grooves [41], and hybrid metal–semiconductor structures [42], have been investigated.

The ability to concentrate light to arbitrarily small dimensions opens the door to both strong coupling with quantum emitters and the construction of compact photonic circuits. Two major challenges must be addressed to realize these goals. First, the momentum mismatch between SPPs and free-space photons makes it difficult to couple into and out of SPP modes from the far field. Many studies rely on natural but inefficient scattering centers in plasmonic waveguides, such as imperfections in the metal film or the ends of the waveguide [43]–[45]. Others utilize near-field scanning optical microscopy (NSOM) to characterize propagation [41], [46]: in this case, however, excitation and collection efficiencies are limited by the transmission through subwavelength apertures [47]. Recently, this limitation has been circumvented by higher efficiency coupling schemes involving near-field detection with electrical components [43] or evanescent coupling to photonic waveguides and fibers [48]. Alternatively, far-field collection has also been improved via gratings designed for directional outcoupling. Second, the losses in metallic systems limit propagation lengths for confined modes, making it difficult to construct resonant cavities and integrated circuits. Some progress has recently been made in exploring new waveguide geometries with lower losses, as well as plasmonic devices incorporating gain media.

In this paper, we will explore recent advances in quantum plasmonics, specifically, efforts toward efficient coupling between quantum emitters and plasmonic waveguides/devices (see Section II), as well as efforts to manipulate and control the resultant SPPs. We will discuss waveguides and integrated plasmonic/photonic devices in Section III, near-field electrical interfaces in Section IV, and active devices in Section V. The final section will present several applications of quantum plasmonics. We primarily examine research and devices relevant to building up quantum plasmonic circuit elements, and review potential applications and strategies for realizing fully functional circuits. For other applications of plasmonic devices outside of the scope of this paper, we refer the reader to several other comprehensive reviews on the topic in [10]–[13], and [38].

II. Coupling to Quantum Emitters

A. *Efficient Coupling of Single Photons to SPPs*

There have been several recent demonstrations of the efficient coupling of quantum emitters to plasmonic waveguides [36]. In 2008, Akimov *et al*. showed that emission from a single quantum emitter could be efficiently coupled into plasmons by positioning colloidal quantum dots near silver nanowire waveguides [see Fig. 2(a)] [45]. The coupling efficiency was estimated to be around 60%, and the emission rate showed a small Purcell enhancement of 1.5–2. Subsequently, Kolesov *et al*. coupled diamond nanocrystals containing nitrogen vacancy (NV)

centers to silver nanowires [see Fig. 2(b)], and showed Fabry–Perot fringes in the SPP-coupled fluorescence, as well as a moderate Purcell enhancement [49]. Other examples include emission enhancement near metal nanoparticles [50], quenching and emission enhancement of single emitters near metallic structures [51]–[54], pumping single emitters from plasmon waveguides [55], enhancement of magnetic dipole transitions near a gold mirror [56], and directing the emission of a single quantum dot to the far field using plasmonic antennas [57].

In most devices, however, it has been difficult to quantify the emission rate enhancement into surface plasmons because lifetime measurements include both radiative and nonradiative contributions, and coupling efficiencies to the far field are difficult to measure accurately. This is of particular concern in plasmonic systems because the nonradiative decay rate can be significantly enhanced very close to the metal surface, leading to an optimum emitter-surface distance for coupling into SPPs that is difficult to control (see Section II-B) [7]. It is therefore important to design experimental schemes to carefully disentangle the nonradiative and radiative emission rates.

B. Purcell Enhancement of Spontaneous Emission

In the weak-coupling regime, the rate of spontaneous emission of a quantum emitter is given by Fermi's golden rule: $\Gamma = 2\pi g^2 \int \rho_e(\omega)\rho_c(\omega)d\omega$ where g is the coupling between the emitter and the electromagnetic field (vacuum Rabi frequency), $\rho_e(\omega)$ is the optical density of states of the emitter at the frequency ω, and $\rho_c(\omega)$ is the optical density of states of the electromagnetic environment. The Rabi frequency is given by $g = \mu\sqrt{\frac{\omega}{\varepsilon_0 \hbar V}}$ where μ is the transition dipole moment of the transition, and V is the mode volume. V is given by $V = (\frac{\lambda_0}{n})^3 \frac{\int \varepsilon |E|^2 dV}{\max(\varepsilon |E|^2)}$, where λ_0 is the free-space wavelength. Some care must be taken in rigorous mode volume calculations in these systems [58], [59]. For a medium with negative dielectric constant, appropriate approximations must be used to avoid negative energy density terms. Typically, the dielectric constant in a dispersive medium is substituted with the "effective dielectric constant" $\varepsilon' = \frac{d(\omega\varepsilon)}{d\omega}$, and the Drude model result for this effective dielectric constant is adequate for order of magnitude estimates.

In a cylindrical plasmonic waveguide with radius R and length L, the effective mode volume is proportional to the mode area, $V_{\text{eff}} \sim R^2 L$. The density of states for plasmonic modes is given by $p(\omega) \sim L \cdot dk/d\omega$, and is inversely proportional to the group velocity. The momentum of SPPs, and thus the group velocity reduction, scales inversely with radius, $k_{\text{SPP}} \sim 1/R$, yielding the scaling relation for emission rate into SPPs, $\Gamma_{\text{SPP}} \propto 1/R^3$.

There can also be enhancement of nonradiative contributions to the emission rate. This has a distance dependence $\frac{\Gamma_{\text{nonrad}}}{\Gamma_0} \approx \frac{3}{16 k_0^3 (d-R)^3 \varepsilon_d^{3/2}} \text{Im}(\frac{\varepsilon_m - 1}{\varepsilon_m + 1})$ and thus there exists an optimum distance from the surface of the plasmonic waveguide to achieve maximum Purcell enhancement [6], [60].

In a plasmonic cavity, this Purcell factor can be further enhanced. Starting from the Purcell enhancement in a cavity $\Gamma = \Gamma_0 \frac{3}{4\pi^2} \frac{Q}{V_{\text{eff}}}$, where Γ_0 is the emission rate in vacuum, we can also write the mode volume in terms of the effective area of the mode A_{eff} and the length of the cavity L_{eff}, $V_{\text{eff}} \sim A_{\text{eff}} L_{\text{eff}}$. If the losses are dominated by material absorption, as expected for plasmonic devices, we can write Q in terms of the SPP propagation length L_{SPP} and SPP wavelength λ_{SPP}, $Q = 2\pi L_{\text{SPP}}/\lambda_{\text{SPP}}$. L_{eff} can be chosen to be as small as $\lambda_{\text{SPP}}/2$. Since λ_{SPP} and L_{SPP} both scale with R, the overall scaling of the Purcell enhancement factor ($F = \Gamma/\Gamma_0$) goes as $1/R^3$. The finesse of the plasmon cavity $\Im$ is given by $L_{\text{SPP}}/L_{\text{eff}}$. Because $\lambda_{\text{SPP}} \sim v_g$, the Purcell enhancement in the plasmonic cavity F can be written as a product of the enhancement due to the bare wire F_0 and $\Im$, $F \propto F_0 \Im$. This intuitive result shows that the electric field confinement is due to the smaller effective area of the mode, and the Purcell factor can be further increased by a factor of the number of roundtrips in the plasmon in the cavity.

C. Color-Selective Single Photon Emission

When an emitter with emission rate Γ_0 is incoherently broadened such that its bandwidth $\Delta\omega > 1/\Gamma_0$, and is coupled to a cavity mode with decay rate $\kappa = \omega/Q < \Delta\omega$, the total emission rate is given by $\Gamma = \Gamma_{\text{freespace}} + \Gamma_{\text{cavity}} = \Gamma_0 + \Gamma_0 \frac{g^2}{\kappa\Gamma_0} \frac{\kappa}{\Delta\omega}$ [61]. The κ terms cancel in this bad emitter limit; increasing the Q of the cavity will increase emission at the resonance frequency, but over a narrower range. For the emission into the cavity mode to be greater than the emission into free space, the condition $g^2/\Gamma_0\Delta\omega > 1$ should be satisfied. An enhancement of the overall emission rate therefore requires that g be increased, which can be achieved only by decreasing V_{eff}. In this broadband emitter regime, small mode volume cavities offer the only means to achieve efficient single photon sources in which the color of emission can be selected, and the emission rate into that mode can be enhanced over emission into free space. Plasmonic cavities therefore provide a unique way to take a broadband quantum emitter and create a color-selectable single photon source. Color-selective single photon sources can have broad applications in quantum information and quantum cryptography.

III. Manipulating SPP Propagation

A. Plasmonic Waveguides and Gratings

A wide variety of plasmonic waveguides have been explored in recent years. The simplest SPP waveguide is a metal surface. The electromagnetic excitation is confined to the surface, decaying evanescently on a scale similar to the plasmon wavelength. In this case, however, confinement can only be achieved at frequencies close to the material plasmon resonance, and the degree of confinement is therefore determined by intrinsic material properties. Furthermore, shorter plasmon wavelengths are accompanied by higher losses in the metal, limiting the utility of this geometry.

It is possible to geometrically engineer confinement at lower frequencies by limiting plasmon propagation to one dimension.

In the quasi-static regime where the electric fields are essentially uniform across a structure at any given time, SPPs can be spatially confined to the dimension of the waveguide. For a 1-D structure such as a cylindrical wire, the radius provides the relevant scaling parameter, and propagating SPPs can be arbitrarily confined to this scale [6], [7], [62]. Unlike schemes in which the localized plasmon resonance is tuned by the nanoparticle shape, this confinement can be broadband, and emission into the plasmon modes can be guided to other parts of the photonic circuit, such as low-loss dielectric waveguides.

As an example, we will examine the case of a subwavelength, metallic, cylindrical wire surrounded by dielectric [7]. As in the case of a flat surface, the momentum along the waveguide is greater than the free-space momentum, $k_{\mathrm{SPP}||} > k_0$. The perpendicular component of momentum is given by momentum conservation: $k_{\mathrm{SPP}\perp} = \sqrt{k_0^2 - k_{\mathrm{SPP}||}^2}$. Therefore, $k_{\mathrm{SPP}\perp}$ is purely imaginary, indicating that the field decays evanescently from the metal surface. The modes can be characterized by their winding number m, an integer that parameterizes their angular momentum around the wire. As the radius of the wire shrinks ($k_{\mathrm{SPP}} R \ll 1$), higher order modes with $m > 1$ exhibit cutoff [see Fig. 1(b)]. The $m = 1$ mode is similar to the fundamental mode of a dielectric waveguide and exists for arbitrarily small radii, but becomes exponentially unconfined. The $m = 0$ fundamental mode has a unique scaling $k_{\mathrm{SPP}||} \sim 1/R$, indicating that the wavelength of SPPs in this mode becomes shorter with decreasing nanowire radius. The propagation length in this mode in units of the plasmon wavelength ($\lambda_{\mathrm{SPP}} = 2\pi/k_{\mathrm{SPP}}$) is given by the ratio of the real and imaginary parts of k_{SPP} ($\mathrm{Re}\, k_{\mathrm{SPP}}/\mathrm{Im}\, k_{\mathrm{SPP}}$). This ratio decreases with decreasing R, but does not go to zero. For example, for silver at $\lambda_0 = 1\ \mu$m, the ratio approaches 140 [see inset of Fig. 1(b)]. Correspondingly, $k_{\mathrm{SPP}\perp} \sim 1/R$, and the mode is increasingly confined in the transverse direction as the radius shrinks.

For a given waveguide radius, there are two competing effects on the confinement as the wavelength increases. As the wavelength is tuned to the red of the plasmon resonance, the confinement due to material dispersion decreases. However, as the wavelength becomes large compared to the radius, the mode area is still set by the size of the nanowire, so the mode volume normalized to the free space wavelength decreases, and thus the field confinement increases. In 1-D systems, it has been shown that the net effect is an increase in confinement at longer wavelengths for gold and silver, leading to potentially greater Purcell enhancement for an emitter placed next to the waveguide [62]. At longer wavelengths, the material losses also decrease, making 1-D plasmonic waveguides especially promising for infrared emitter coupling.

This favorable scaling with shrinking device dimension is general to 1-D systems (see Fig. 3), such as MIM waveguides [40], grooves [11], arrays of metallic dots [39], [64], [65], and hybrid gap plasmons [42], [66], [67]. Hybrid gap plasmons formed by a metal surface and a high index nanowire separated by a small gap are particularly promising, as the mode is pulled away from the metal surface by the high index material, thereby allowing tight field confinement with lower losses.

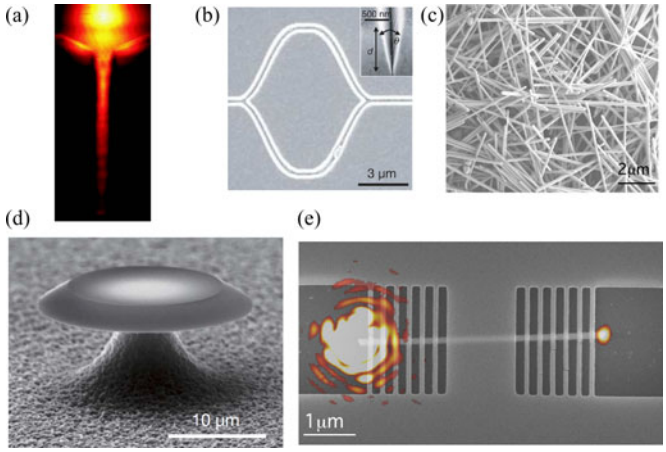

Fig. 3. Plasmonic waveguide and cavity geometries. (a) Propagation down a metal stripe waveguide, characterized by NSOM (reproduced with permission from [46]). (b) Scanning electron microscope (SEM) image of a groove waveguide interferometer (reproduced with permission from [41]). (c) SEM image of chemically synthesized silver nanowires, which can be used as highly crystalline, defect-free 1-D SPP waveguides. (d) SEM image of a whispering gallery mode plasmonic cavity (reproduced with permission from [63]). (e) SEM image of an SPP cavity formed by dielectric gratings around a silver nanowire [61]. Overlay shows far-field transmission characterization. The left-hand spot is the reflected laser spot, and the right-hand spot shows coupling into the far field at the other end of the nanowire.

Surface plasmons can be manipulated, focused, and directed by periodic patterning in the waveguide [10], [13], [41], [68], [69]. A periodic potential of period Λ imparts a lattice momentum $k_{\mathrm{lattice}} = 2\pi/\Lambda$ on the propagating SPPs. Two special cases are commonly employed in devices. For incident SPPs with $k_{\mathrm{SPP}} = 2\pi/\Lambda$, the lattice will act as a mirror, forming the basis for plasmonic-distributed Bragg reflectors. For SPPs with $k_{\mathrm{SPP}} = 2\pi/\Lambda$, the forward momentum becomes $k = 0$, and the excitation is scattered to the far field as photons that propagate nearly perpendicularly to the SPP propagation direction. These gratings can thus be used as directional outcouplers.

Most plasmonic grating designs involve direct patterning and etching of the metal. However, lithographic errors can introduce scattering centers that limit the performance of these structures. Reported examples of plasmonic resonators therefore rely on larger mode volume geometries to reduce scattering losses, as is the case with recently reported plasmonic whispering gallery mode microdisk cavities [see Fig. 3(d)] [63], [70]. Another strategy is to pattern the dielectric component of the metal–dielectric interface [see Fig. 3(e)]. The effective index of the SPP is proportional to the refractive index of the dielectric; therefore, the Bragg condition can be met by alternating layers of dielectric in contact with the metal. This strategy has the advantage that the metal surface can remain smooth and any lithographic imperfections will be present in a lower index dielectric material, thus reducing scattering losses [61].

B. Chemically Synthesized Nanostructures

One strategy for minimizing propagation losses is to utilize chemically synthesized metallic waveguides. Top-down lithographically defined structures can have two major sources of

loss. First, lithographic imperfections can introduce scattering centers. Second, metal films deposited by physical vapor deposition or electrochemical methods are polycrystalline, with grain sizes ranging from few to tens of nanometers. When plasmons encounter these grain boundaries, they can be lost by scattering into free-space as photons or into the material as phonons.

Chemically synthesized structures can be highly crystalline with smooth, defect-free surfaces. Many examples of quantum emitter-SPP coupling have been realized with silver nanowires [see Fig. 3(c)], which are synthesized using a solution-phase polyol process [71]. These 1-D structures are generated by reducing silver nitrate with ethylene glycol in the presence of poly(vinylpyrrolidone) (PVP). The ethylene glycol acts as the solvent and the reducing agent, while the PVP is speculated to coordinate to specific faces of silver to induce growth in one direction. These silver nanowires are typically 50–200 nm in diameter and 1–50 μm long. The wire diameter and length can be tailored by changing the reaction conditions. Propagation lengths at optical frequencies have been reported up to 20 μm [43], [44], [48], which indicates lower losses than one would expect from optical constants reported by Palik [72].

One major limitation of silver nanowires is that they degrade over time. When exposed to ambient conditions, silver oxidizes, and the oxide can photoreduce to form nanoparticles [73]. These act as scattering centers, decreasing plasmon propagation lengths. In addition, silver nanoparticles can fluoresce, problematic for quantum emitter coupling. Efforts to functionalize or otherwise protect the silver surface will be important for future applications.

As a plasmonic waveguide material, gold has higher losses, but has the distinct advantage of being inert and stable. While gold nanoparticle and nanorod syntheses are abundant in the literature, a high-yield method for growing long, highly crystalline, gold nanowires with 50–200 nm diameters has yet to be developed, despite much effort [74]–[79].

C. Plasmonic–Photonic Optical Circuits

The high absorption losses in plasmonic circuits limit their utility for even short distance on-chip communication. The development of hybrid photonic–plasmonic structures is thus critical for realization of optical circuits. The coupling of emission into a silver nanowire and then into an optical fiber has been theoretically calculated to be as high as 95% for optimized nanowire radius [6]. The coupling efficiency shows a peak with respect to nanowire radius, reflecting the balance between emitter/plasmon coupling, SPP propagation losses, and the wave vector mismatch. Experimentally, coupling efficiencies to optical fibers as high as 55% have been reported [80]. Similarly, coupling efficiencies between silver nanowires and dielectric nanowires as high as 56% have been observed [48]. Scalable approaches, such as coupling to polymer waveguides [81], will be important for future applications.

IV. Near-Field Electrical Interfaces

One strategy for increasing the excitation and detection efficiency in plasmonic devices is to engineer electrical interfaces in the near field. SPPs can be converted to excitons in a semiconductor, and the resultant charges can be separated and collected in an electrical circuit. Falk *et al*. demonstrated in 2009 that a simple cross bar of a plasmonic waveguide and a semiconductor nanowire forms a Schottky junction, and the built-in electric field at that junction can be used to separate charges at zero bias [see Fig. 4(a)] [43]. The detection efficiency can be as high as 10% at zero bias, and at finite bias, while charge traps in the nanowire provide an additional "gate field," resulting in gain of the electrical signal of up to 50 electrons/plasmon. This device geometry was sensitive enough to detect emission from a single quantum dot coupled to the silver nanowire (see Fig. 5). A similar implementation used an MIM waveguide on top of a GaAs active region, in which the charges were separated at the Schottky barrier formed by the gold-GaAs contact [see Fig. 4(b)] [82]. More recent demonstrations have made use of tunneling at the metal–semiconductor Schottky barrier to map LSPs in optical antennas [83], [84].

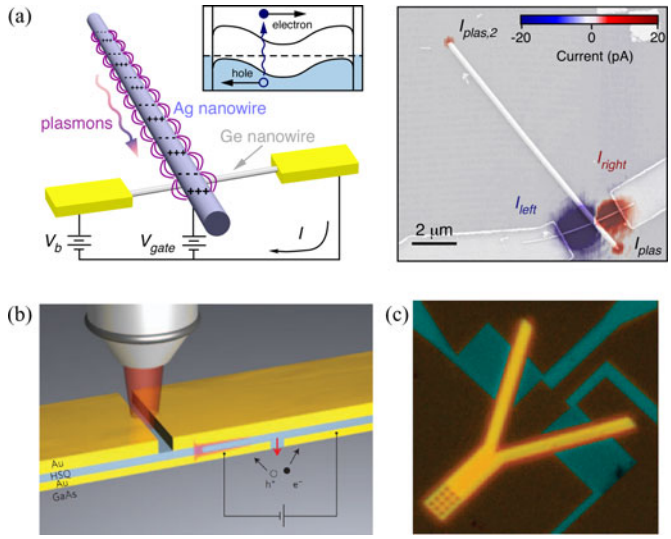

Fig. 4. Electrical interfaces for SPPs. (a) Cross-bar structure with a silver nanowire plasmonic waveguide and a Ge semiconducting nanowire. SPPs convert to electron–hole pairs at the interface, which are then detected as current. (Right) Scanning photocurrent image with SEM overlay showing photocurrent originating from direct excitation of electron–hole pairs, as well as indirect excitation via scattering into SPPs at the ends of the silver nanowire (reproduced with permission from [43]). (b) Schematic of a gap plasmon waveguide/semiconductor device (reproduced with permission from [82]). (c) SEM of a plasmonic waveguide beamsplitter coupled to two superconducting detectors (reproduced with permission from [85]). Such schemes are fast enough to do direct photon statistics measurements electrically.

Another scheme for electrical detection of plasmons is coupling the plasmonic waveguide to a superconducting detector [see Fig. 4(c)] [85]. The superconducting NbN wire is biased close to the critical current regime such that absorption of a single photon or SPP causes a section of the wire to become normal. The resulting resistance is detected electrically. This technique has the distinct advantage of being fast, with detector dead times of less than 10 ns. Indeed, when a superconducting wire was used to detect photons in an integrated photonic circuit, the detection was fast enough to resolve the transit time of single photons around a ring resonator [86]. By comparison,

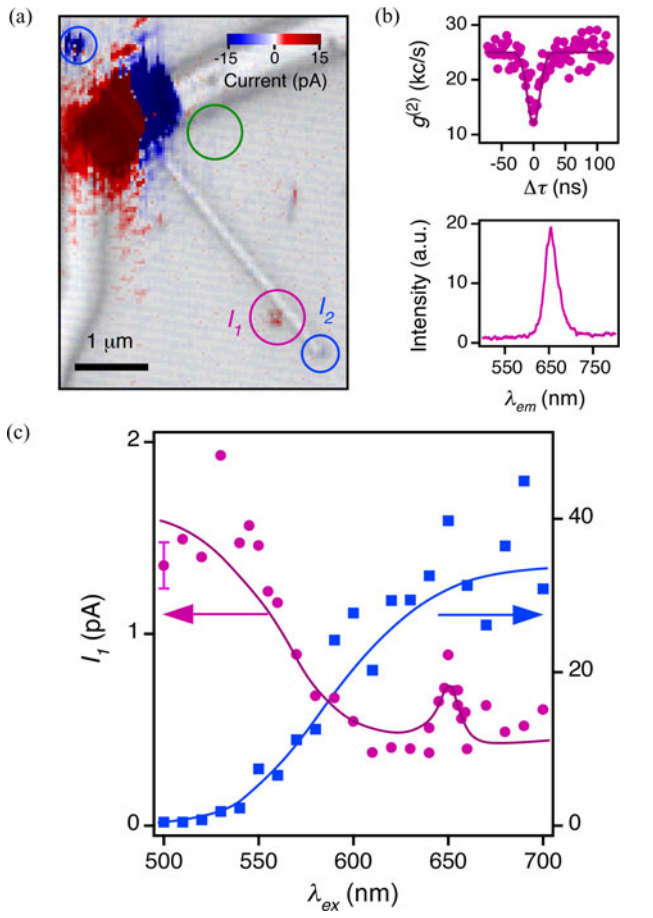

Fig. 5. Electrical detection of a single quantum dot [43]. (a) Scanning photocurrent image showing electrical detection of SPPs from the ends of the silver nanowire plasmon waveguide (blue circles) and a quantum dot (pink circle). Other quantum dots that are not coupled to the waveguide identified by fluorescence mapping do not appear in the photocurrent map (green circle). (b) Photon correlation statistics (top) show that this quantum dot is a single photon source, and the fluorescence spectrum (bottom) looks characteristic of a single CdSe quantum dot of this size. (c) Electrical detection current as a function of excitation wavelength, exciting from the end of the waveguide (blue) and at the quantum dot (pink). The signal increases as a function of wavelength for the waveguide-coupled spot, and shows a characteristic exciton peak for the quantum dot-coupled spot.

the semiconductor nanowire detector in [43] was limited to ~30 kHz operation. Superconducting detectors are fast enough to perform autocorrelation measurements, and this feature was used to unambiguously prove detection of single SPPs.

Reciprocally, inelastic scattering of charges traversing the Schottky junction can be used to generate surface plasmons [87]. In a semiconductor nanowire-silver nanowire cross bar, a voltage can be applied across the junction, resulting in electroluminescence. Similar to the emission rate enhancement of a dipole next to a nanoscale plasmonic waveguide, the decay of electron–hole pairs in the semiconductor can be enhanced and efficiently coupled into SPP modes of the silver nanowire. The resultant SPPs can then be collected electrically by another semiconductor nanowire-silver nanowire junction.

In a similar demonstration of electrical excitation of SPPs, a tunneling current from an atomic force microscope (AFM) tip was used to inject electrons into a gold nanowire that inelastically scattered to excite LSPs, which subsequently coupled to SPPs [88]. Another study showed the coupling of electroluminescence of Si nanoparticles to gap plasmon modes in an MIM waveguide [89]. All of these examples suffer from the use of a highly inefficient photon source. The next step in near-field excitation will be the efficient coupling of excitons into SPPs from a LED or quantum well structure [90], [91].

V. Active Devices

A. Plasmonic Waveguides With Modulation and Gain

One way to compensate for losses in a metallic waveguide is to surround the waveguide with an active gain medium. There have been a number of examples of active plasmonic devices in which plasmon propagation is modulated by optical or electrical switching of another medium, such as exploiting the structural phase transition of gallium [92], using the thermo-optic effect [93], optical excitation of photochromic molecules [94], electrically pumping an Si layer in a transistor geometry [95], and optically pumping thin films of colloidal quantum dots [96]. More recently, net gain in a plasmonic waveguide was achieved by optically pumping a fluorescent dye [97]. All of these device geometries, however, suffer from relatively long switching times in the tens of nanoseconds to microsecond range. One recent demonstration showed that femtosecond switching times could be achieved by optically switching the free carrier density in aluminum, leading to a few percent modulation in the SPP signal, opening the door to plasmonic circuits with terahertz bandwidths [98].

B. Plasmonic Lasers

The large enhancement factors in plasmonic systems open the tantalizing prospect of lasing into surface plasmon modes, confined to deep subwavelength scales. Plasmonic lasers (often called SPASERs for "surface plasmon amplification by stimulated emission of radiation") were proposed in 2003 by Bergman and Stockman [99], and were first realized in LSP modes of a gold nanoparticle coated in dye-doped silica [100]. A subsequent demonstration using gap mode SPPs between a CdS nanowire and a silver film showed a high β factor (the percentage of emission into a single mode) into the lasing mode [66]. A more recent experiment from the same group achieved room temperature operation by use of a gap mode between a CdS square and a silver film [101].

These preliminary steps have demonstrated that the losses in plasmonic modes can indeed be overcome, and that plasmonic lasers can potentially be the smallest lasers; however, they have yet to demonstrate any key functional advantages over conventional lasers. One possible advantage is that the high Purcell enhancement and thus high β factor into plasmonic modes can enhance the lasing efficiency, and could lead to low threshold or thresholdless lasers [102]. Furthermore, the emission enhancement is intrinsically broadband in nature, leading to lasers that can operate at much lower quality factors. The next steps in plasmonic lasers will be to find new geometries and new

materials to exploit these advantages, as well as new schemes for electrically pumped plasmon lasers.

VI. Quantum Information Processing

A. Cavity Quantum Electrodynamics (QED) With Plasmonic Cavities

In the strong coupling regime of cavity QED, the coupling strength between the cavity and the emitter exceeds dissipation into the environment. For some applications, such as efficient generation of single SPPs, it is sufficient that $g^2 > \kappa\Gamma_0$. As defined previously, g is the vacuum Rabi frequency, κ is the cavity loss rate, and Γ_0 is the bare emission rate into free space. When $g > \kappa, \Gamma_0$, other interesting physics can also be explored. In this regime, an excitation can be reversibly transferred between the cavity and the emitter, resulting in Rabi oscillations. Although there have been several demonstrations of the former condition [45], [49], [61], which corresponds to a Purcell factor $\sim$1, achieving low enough losses (small κ) is a very challenging task due to the high intrinsic losses in plasmonic systems. For a typical emitter, $\Gamma_0 \sim 10$ MHz. The lowest achievable κ is set by the plasmon propagation length, which is typically 100–200 λ_{SPP}, corresponding to a $\kappa \sim 10$ THz. For mode volumes of $0.01(\lambda/n)^3$, $g \sim 100$ GHz. In order to achieve $g > \kappa$, the coupling strength therefore needs to be at least 100 times higher than in previous demonstrations. Considering typical losses in the optical range, a plasmonic cavity with a mode volume of $10^{-4}(\lambda/n)^3$ is required for this purpose.

Devices of this size have not yet been demonstrated, but are within reach of existing schemes. For the plasmonic cavity in [61], the Purcell factor scales as $1/R^3$, and strong coupling can thus be obtained with silver nanowires of diameter $\sim$20 nm. Excitation and detection in the far field would be very difficult at these scales, so near-field interfaces to either photonic waveguides or electrical interfaces would be crucial.

Another possibility is to utilize plasmonic modes that are pulled away from the metallic substrate while still maintaining confinement, as in gap plasmon structures [42], [66]. These modes can have lower losses for the same confinement. In addition, in 1-D waveguide geometries, one can achieve lower losses and higher confinement in the infrared. Investigations in this spectral range are limited due to the lack of availability of good emitters. At near IR wavelengths, however, there exist a number of promising candidates such as lead salt quantum dots [103] and InGaAs epitaxial quantum dots [104].

B. Photon–Photon Interactions

A photonic transistor is a device in which an optical "gate" field controls the propagation of another optical field via a nonlinear interaction, analogous to an electronic transistor. Such a device has been extremely difficult to realize because single-photon nonlinearities are typically very weak. There are many schemes currently being explored for controlling and enhancing nonlinearities at the single-photon level, such as nonlinearities in atomic ensembles [105]–[107] and coupling single atoms to high finesse cavities [108]–[110]. One possible strategy to accomplish this goal in the solid state is to use the strong coupling between single photon emitters and SPPs [111].

We will consider the proposed scheme in [111] in detail. A two-level emitter coupled to a SPP waveguide can act as a saturable mirror. For large Purcell factors F, the reflection $r \sim -(1 - 1/F)$ approaches unity, and emission rate to the far field is suppressed, $\Gamma = 1 - R - T = 2R/F$. This picture holds for low powers, but as the transition becomes saturated, transmission again approaches unity. This phenomenon should be evident in the photon statistics of the transmitted and reflected photons: the second-order correlation function $g^{(2)}(t)$ of reflected photons should be antibunched at $t = 0$, while that of the transmitted photons should be bunched at $t = 0$. At higher powers, $g^{(2)}(t)$ for the transmitted photons approaches unity at all times. This phenomenon is known as "photon blockade," and is distinct from previous demonstrations with a single atom coupled to a high finesse cavity [108], in which the transmission characteristics of the cavity are determined entirely by the anharmonic spectrum of the dressed atom, and there can only be transmission at multiphoton resonances of the atom-cavity system.

A similar scheme can be used to realize the single photon transistor. In this case, a three-level emitter is coupled to an SPP waveguide: one transition ($|\mathrm{e}> - |\mathrm{g}>$) is strongly coupled to the SPPs, while the other ($|\mathrm{e}> - |\mathrm{s}>$) is decoupled [see Fig. 6(a)]. If the emitter is in $|\mathrm{g}>$, the system has the properties of the saturable mirror. If the emitter is in $|\mathrm{s}>$, photons will be transmitted, as the ($|\mathrm{e}> - |\mathrm{s}>$) transition is decoupled from the surface plasmons. Thus, a control field driving the ($|\mathrm{e}> - |\mathrm{s}>$) transition can be used to control whether the emitter reflects or transmits photons with unity probability. The effective "gain" of the transistor is given by the number of photons that can be reflected or transmitted before an undesirable state change occurs, which is approximately given by F.

As with other applications, it is critical to develop integrated photonic or electronic interfaces to enable the single photon transistor. The inevitable tradeoff between high Purcell factors and losses at greater confinement factors can be ameliorated by the integration of low-loss waveguides.

C. Nanoscale Atom Traps

There is currently much interest in trapping and manipulating atoms close to surfaces for quantum information processing [112]. Such hybrid systems could combine the long coherence times and narrow transitions of atoms with the scalability and high collection efficiencies of integrated photonics. The primary challenge in realizing such systems is the integration between atoms and other structures, since atoms or ions must be confined far enough away from the surface to retain their favorable properties, but must be close enough for their emission to couple efficiently. This is particularly difficult because strong van der Waals forces pull the atom or ion into the surface, and trapped charges can lead to patch potentials that dephase ions [113]. One potential route to hybrid systems is to use the plasmonic waveguide itself for trapping [see Fig. 6(b)]: the large electric field gradients at a nanoscale tip can be used to trap sin-

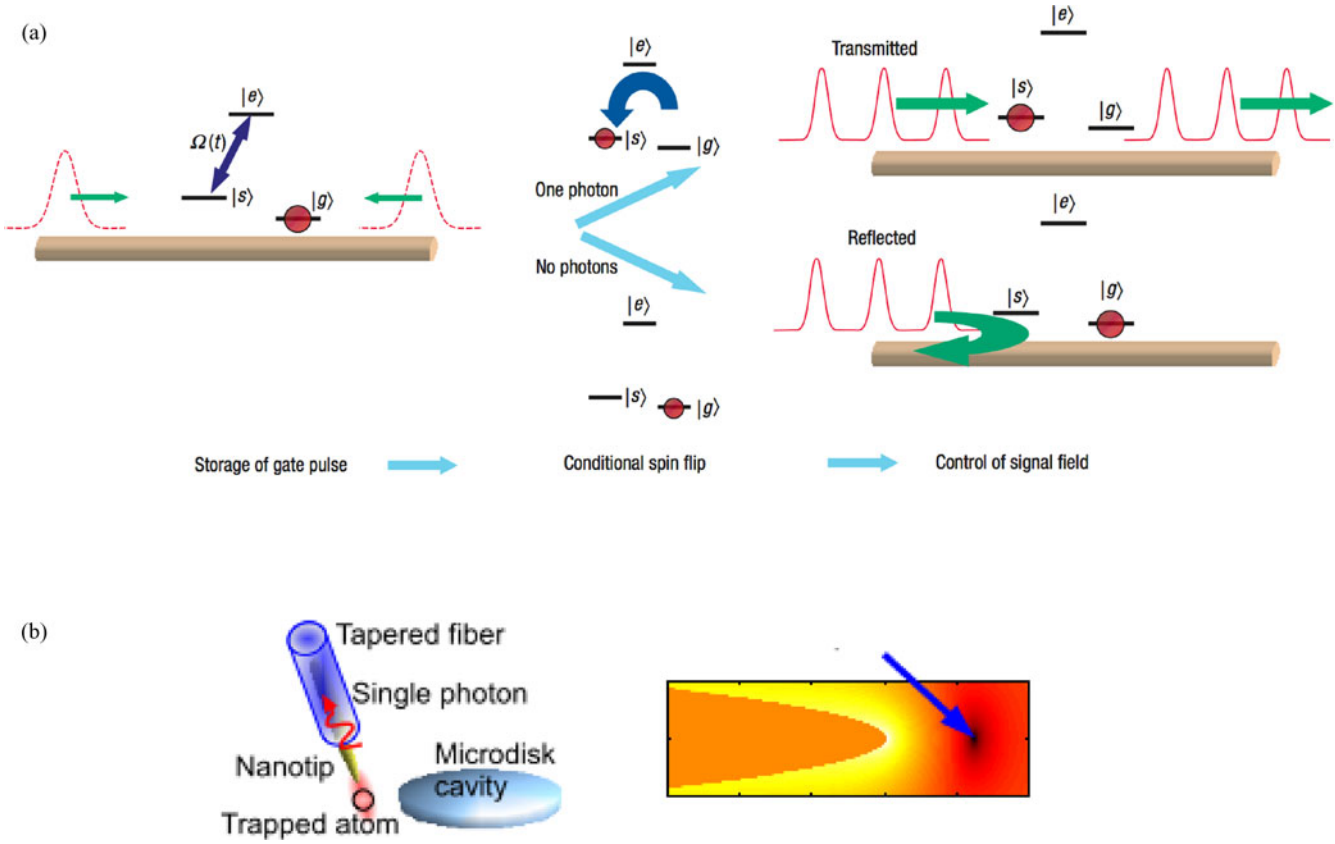

Fig. 6 (a) Scheme for a single photon transistor with SPPs (reproduced with permission from [111]). A single SPP is either transmitted or reflected depending on the state of a quantum emitter coupled to the SPP waveguide. (b) Schematic of an integrated nanotrap for atoms using the tip of a plasmonic nanowire (reproduced with permission from [60]). A plasmonic nanowire is adiabatically coupled to a tapered fiber, which can allow for highly efficient collection of SPPs into photons. This atom can be scanned near other structures, such as the microdisk cavity depicted. (Right) Electric field intensity profile near the tip of a nanowire. An intensity minimum (indicated by the blue arrow) results from destructive interference between the incident and reflected plane wave, and can act as a nanoscale atom trap.

gle atoms, and the high Purcell enhancement into SPP modes can be used to manipulate the atom and efficiently collect single photons [60]. A recent preliminary study showed interaction between a Bose–Einstein condensate and surfaces potentials in the near field of a plasmonic waveguide [114], but plasmonic trapping of atoms has yet to be demonstrated experimentally.

When a sharp, metallic nanotip is excited by an incident plane wave, the negative dielectric constant of the metal leads to destructive interference between the excitation and the reflection [60]. This destructive interference can thus create a potential minimum close to the tip, which acts as a trap when blue-detuned from an atomic transition. This trap can have deep subwavelength dimensions and large trap frequencies.

An atom trapped at the tip of a nanowire can be strongly coupled to SPPs that propagate along the wire. The atom can thus be optically manipulated and read out via surface plasmons with high efficiency. The effective Purcell enhancement F into SPP modes depends largely on the tip size, and $F > 1$ can be achieved for $\sim$ 1-nm tip curvatures. For efficient collection, the metallic nanowire can be coupled to a tapered optical fiber, where single SPPs can be efficiently converted to single photons.

VII. Conclusion

Plasmonic devices are a promising platform for quantum information processing, and provide a natural platform for high bandwidth nanoscale quantum circuits. They can be used to achieve extraordinarily strong light–matter interactions, and, crucially, they exhibit favorable scaling as their dimensions shrink deep below the diffraction limit. There are several applications for which the small mode volumes achievable only with plasmonic systems are critical, such as color-selective single photon emission, thresholdless lasing, and nanoscale photonic circuits. However, the field is still in its infancy, and much work needs to be done toward engineering and optimizing new plasmonic mode geometries, as well as near-field electrical and optical interfaces, and integrating these systems in order to realize the full potential of these applications.

Acknowledgment

The authors would like to thank B. Shields, J. Thompson, and J. Robinson for helpful discussions.

REFERENCES

[1] M. O. Scully and M. S. Zubairy, *Quantum Optics*. Cambridge, U.K.: Cambridge Univ. Press, 1997.

[2] S. J. van Enk and H. J. Kimble, "Strongly focused light beams interaction with single atoms in free space," *Phys. Rev. A*, vol. 63, pp. 023809-1–023809-11, 2001.

[3] G. Wrigge, I. Gerhardt, J. Hwang, G. Zumofen, and V. Sandoghdar, "Efficient coupling of photons to a single molecule and the observation of its resonance fluorescence," *Nature Phys*., vol. 4, pp. 60–66, 2007.

[4] M. K. Tey, Z. Chen, S. A. Aljunid, B. Chng, F. Huber, G. Maslennikov, and C. Kurtsiefer, "Strong interaction between light and a single trapped atom without the need for a cavity," *Nature Phys*., vol. 4, pp. 924–927, 2008.

[5] K. Vahala, "Optical microcavities," *Nature*, vol. 424, pp. 839–846, 2003.

[6] D. E. Chang, A. S. Sorensen, P. R. Hemmer, and M. D. Lukin, "Quantum optics with surface plasmons," *Phys. Rev. Lett*., vol. 97, pp. 053002-1–053002-4, 2006.

[7] D. E. Chang, A. S. Sorensen, P. R. Hemmer, and M. D. Lukin, "Strong coupling of single emitters to surface plasmons," *Phys. Rev. B*, vol. 76, pp. 035420-1–035420-26, 2007.

[8] G. Mie, "Considerations on the optics of turbid media, especially colloidal metal sols," *Ann. Phys*., vol. 25, pp. 377–442, 1908.

[9] R. H. Ritchie, "Plasma losses by fast electrons in thin films," *Phys. Rev.*, vol. 106, pp. 874–881, 1957.

[10] W. L. Barnes, A. Dereux, and T. W. Ebbesen, "Surface plasmon subwavelength optics," *Nature*, vol. 424, pp. 824–830, 2003.

[11] D. K. Gramotnev and S. I. Bozhevolnyi, "Plasmonics beyond the diffraction limit," *Nature Photon*., vol. 4, pp. 83–91, 2010.

[12] E. Ozbay, "Plasmonics: Merging photonics and electronics at nanoscale dimensions," *Science*, vol. 311, pp. 189–193, 2006.

[13] J. A. Schuller, E. S. Barnard, W. Cai, Y. C. Jun, J. S. White, and M. L. Brongersma, "Plasmonics for extreme light concentration and manipulation," *Nature Mater.*, vol. 9, pp. 193–204, 2010.

[14] M. L. Brongersma and V. M. Shalaev, "The case for plasmonics," *Science*, vol. 328, pp. 440–441, 2010.

[15] N. R. Jana, L. Gearheart, and C. J. Murphy, "Wet chemical synthesis of high aspect ratio cylindrical gold nanorods," *J. Phys. Chem. B*, vol. 105, pp. 4065–4067, 2001.

[16] M. Liu and P. Guyot-Sionnest, "Mechanism of silver(I)-assisted growth of gold nanorods and bipyramids," *J. Phys. Chem. B*, vol. 109, pp. 22192–22200, 2005.

[17] R. D. Averitt, D. Sarkar, and N. J. Halas, "Plasmon resonance shifts of Au-coated Au2S nanoshells: Insight into multicomponent nanoparticle growth," *Phys. Rev. Lett*., vol. 78, pp. 4217–4220, 1997.

[18] C. Graf and A. von Blaaderen, "Metallodielectric colloidal core-shell particles for photonic applications," *Langmuir*, vol. 18, pp. 524–534, 2002.

[19] J. Aizpurua, P. Hanarp, D. S. Sutherland, M. Kall, G. W. Byrant, and F. J. Garcia de Abajo, "Optical properties of gold nanorings," *Phys. Rev. Lett*., vol. 90, pp. 057401-1–057401-4, 2003.

[20] F. Kim, S. Connor, H. Song, T. Kuykendall, and P. Yang, "Platonic gold nanocrystals," *Angew. Chem*., vol. 116, pp. 3759–3763, 2004.

[21] Y. Sun and Y. Xia, "Shape-controlled synthesis of gold and silver nanoparticles," *Science*, vol. 298, pp. 2176–2179, 2002.

[22] A. R. Tao, S. Habas, and P. Yang, "Shape control of colloidal metal nanocrystals," *Small*, vol. 4, pp. 310–325, 2008.

[23] S. R. Nicewarner-Pena, R. G. Freeman, B. D. Reiss, L. He, D. J. Pena, I. D. Walton, R. Cromer, C. D. Keating, and M. J. Natan, "Submicrometer metallic barcodes," *Science*, vol. 294, pp. 137–141, 2001.

[24] L. Novotny and N. van Hulst, "Antennas for light," *Nature Photon*., vol. 5, pp. 83–90, 2012.

[25] T. W. Ebbesen, H. J. Lezec, H. F. Ghaemi, T. Thio, and P. A. Wolff, "Extraordinary optical transmission through sub-wavelength hole arrays," *Nature*, vol. 391, pp. 667–669, 1998.

[26] C. Zhu, H. Liu, S. M. Wang, T. Li, J. X. Cao, Y. J. Zheng, L. Li, Y. Wang, S. N. Zhu, and X. Zhang, "Electric and magnetic excitation of coherent magnetic plasmon waves in a one-dimensional meta-chain," *Opt. Exp*., vol. 18, pp. 26268–26273, 2010.

[27] A. Tao, P. Sinsermsukasakul, and P. Yang, "Tunable plasmonic lattices of silver nanocrystals," *Nature Nanotechnol*., vol. 2, pp. 435–440, 2007.

[28] J. A. Fan, C. Wu, K. Bao, J. Bao, R. Bardhan, N. J. Halas, V. N. Manoharan, P. Nordlander, G. Shvets, and F. Capasso, "Self-assembled plasmonic nanoparticle clusters," *Science*, vol. 328, pp. 1135–1138, 2010.

[29] E. Prodan, C. Radloff, N. J. Halas, and P. Nordlander, "A hybridization model for the plasmon response of complex nanostructures," *Science*, vol. 302, pp. 419–422, 2003.

[30] S. Nie and S. R. Emory, "Probing single molecules and single nanoparticles by surface-enhanced Raman scattering," *Science*, vol. 275, pp. 1102–1106, 1997.

[31] N. Liu, M. L. Tang, M. Hentschel, H. Giessen, and A. P. Alivisatos, "Nanoantenna-enhanced gas sensing in a single tailored nanofocus," *Nature Mater.*, vol. 10, pp. 631–636, 2011.

[32] H. A. Atwater and A. Polman, "Plasmonics for improved photovoltaic devices," *Nature Mater.*, vol. 9, pp. 205–213, 2010.

[33] M. Liu, N. de Leon Snapp, and H. Park, "Water photolysis with a cross-linked titanium dioxide nanowire anode," *Chem. Sci*., vol. 2, pp. 80–87, 2011.

[34] Z. Liu, W. Hou, P. Pavaskar, M. Aykol, and S. B. Cronin, "Plasmon resonant enhancement of photocatalytic water splitting under visible illumination," *Nano Lett*., vol. 11, pp. 1111–1116, 2011.

[35] J. A. Fan, K. Bao, C. Wu, J. Bao, R. Bardhan, N. J. Halas, V. N. Manoharan, G. Shvets, P. Nordlander, and F. Capasso, "Fano-like interference in self-assembled plasmonic quadrumer clusters," *Nano Lett*., vol. 10, pp. 4680–4685, 2010.

[36] D. E. Chang, "Controlling atom-photon interactions in nano-structured media," Ph.D. dissertation, Dept. Phys., Harvard University, Cambridge, MA, 2008.

[37] R. Zia, M. D. Selker, P. B. Catrysse, and M. L. Brongersma, "Geometries and materials for subwavelength surface plasmon modes," *J. Opt. Soc. Amer. A*, vol. 21, pp. 2442–2446, 2004.

[38] S. A. Maier, *Plasmonics: Fundamentals and Applications*. New York: Springer, 2007.

[39] S. A. Maier, P. G. Kik, H. A. Atwater, S. Meltzer, A. A. G. Requicha, and B. E. Koel, "Observation of coupled plasmon-polariton modes of plasmon waveguides for electromagnetic energy transport below the diffraction limit," *Proc. SPIE*, vol. 4810, pp. 71–81, 2002.

[40] R. Zia, M. D. Selker, and M. L. Brongersma, "Leaky and bound modes of surface plasmon waveguides," *Phys. Rev. B*, vol. 71, pp. 165431-1–165431-9, 2005.

[41] S. I. Bozhevolnyi, V. S. Volkov, E. Devaux, J.-Y. Laluet, and T. W. Ebbesen, "Channel plasmon subwavelength waveguide components including interferometers and ring resonators," *Nature*, vol. 440, pp. 508–511, 2006.

[42] R. F. Oulton, V. J. Sorger, D. A. Genov, D. F. P. Pile, and X. Zhang, "A hybrid plasmonic waveguide for subwavelength confinement and long-range propagation," *Nature Photon*., vol. 2, pp. 496–500, 2008.

[43] A. L. Falk, F. H. L. Koppens, C. L. Yu, K. Kang, N. d. L. Snapp, A. V. Akimov, M.-H. Jo, M. D. Lukin, and H. Park, "Near-field electrical detection of optical plasmons and single-plasmon sources," *Nature Phys*., vol. 5, pp. 475–479, 2009.

[44] H. Ditlbacher, A. Hohenau, D. Wagner, U. Kreibig, M. Rogers, F. Hofer, F. R. Aussenegg, and J. R. Krenn, "Silver nanowires as surface plasmon resonators," *Phys. Rev. Lett*., vol. 95, pp. 257403-1–257403-4, 2005.

[45] A. V. Akimov, A. Mukherjee, C. L. Yu, D. E. Chang, A. S. Zibrov, P. R. Hemmer, H. Park, and M. D. Lukin, "Generation of single optical plasmons in metallic nanowires coupled to quantum dots," *Nature*, vol. 450, pp. 402–406, 2007.

[46] R. Zia, J. A. Schuller, and M. L. Brongersma, "Near-field characterization of guided polariton propagation and cutoff in surface plasmon waveguides," *Phys. Rev. B*, vol. 74, pp. 165415-1–165415-12, 2006.

[47] H. Heinzelmann and D. Pohl, "Scanning near-field optical microscopy," *Appl. Phys. A*, vol. 59, pp. 89–101, 1994.

[48] R. Yan, P. Pausauskie, J. Huan, and P. Yang, "Direct photonic-plasmonic coupling and routing in single nanowires," *Proc. Nat. Acad. Sci*., vol. 106, pp. 21045–21050, 2009.

[49] R. Kolesov, B. Grotz, G. Balasubramanian, R. J. Stohr, A. A. L. Nicolet, P. R. Hemmer, F. Jelezko, and J. Wrachtrup, "Wave-particle duality of single surface plasmon polaritons," *Nature Phys*., vol. 5, pp. 470–474, 2009.

[50] S. Schietinger, M. Barth, T. Aichele, and O. Benson, "Plasmon-enhanced single photon emission from a nanoassembled metal-diamond hybrid structure at room temperature," *Nano Lett*., vol. 9, pp. 1684–1698, 2009.

[51] P. Maletinsky, S. Hong, M. S. Grinolds, B. Hausmann, M. D. Lukin, R. L. Walsworth, M. Loncar, and A. Yacoby, "A robust, scanning quantum system for nanoscale sensing and imaging," *Engineering*, pp. 1–11, 2011.

[52] A. Cuche, O. Mollet, A. Drezet, and S. Huant, "'Deterministic' quantum plasmonics," *Nano Lett*., vol. 10, pp. 4566–4570, 2010.

[53] A. Huck, S. Kumar, A. Shakoor, and U. L. Andersen, "Controlled coupling of a single nitrogen-vacancy center to a silver nanowire," *Phys. Rev. Lett*., vol. 106, pp. 096801-1–096801-4, 2011.

[54] M. L. Andersen, S. Stobbe, A. S. Sorensen, and P. Lodahl, "Strongly modified plasmon-matter interaction with mesoscopic quantum emitters," *Nature Phys*., vol. 7, pp. 215–218, 2010.

[55] H. Wei, D. Ratchford, X. Li, H. Xu, and C.-K. Shih, "Propagating surface plasmon induced photon emission from quantum dots," *Nano Lett*., vol. 9, pp. 4168–4171, 2009.

[56] S. Karaveli and R. Zia, "Spectral tuning by selective enhancement of electric and magnetic dipole emission," *Phys. Rev. Lett*., vol. 106, pp. 193004-1–193004-4, 2011.

[57] A. G. Curto, G. Volpe, T. H. Taminiau, M. P. Kreuzer, R. Quidant, and N. F. van Hulst, "Unidirectional emission of a quantum dot coupled to a nanoantenna," *Science*, vol. 329, pp. 930–933, 2010.

[58] S. A. Maier, "Effective mode volume of nanoscale plasmon cavities," *Opt. Quantum Electron*., vol. 38, pp. 257–267, 2006.

[59] R. Ruppin, "Electromagnetic energy density in a dispersive and absorptive material," *Phys. Lett. A*, vol. 299, pp. 309–312, 2002.

[60] D. E. Chang, J. D. Thompson, H. Park, V. Vuletic, A. S. Zibrov, P. Zoller, and M. D. Lukin, "Trapping and manipulation of isolated atoms using nanoscale plasmonic structures," *Phys. Rev. Lett*., vol. 103, pp. 123004-1–123004-4, 2009.

[61] N. P. de Leon, B. J. Shields, C. L. Yu, D. Englund, A. V. Akimov, M. D. Lukin, and H. Park, "Tailoring light-matter interaction with a nanoscale plasmon resonator," *Phys. Rev. Lett*., 2012, to be published.

[62] D. A. Genov, R. F. Oulton, G. Bartal, and X. Zhang, "Anomalous spectral scaling of light emission rates in low-dimensional metallic nanostructures," *Phys. Rev. B*, vol. 83, pp. 245312-1–245312-7, 2011.

[63] B. Min, E. Ostby, V. J. Sorger, E. Ulin-Avila, L. Yang, X. Zhang, and K. Vahala, "High-Q surface-plasmon-polariton whispering-gallery microcavity," *Nature*, vol. 457, pp. 455–459, 2009.

[64] S. A. Maier, P. G. Kik, H. A. Atwater, S. Meltzer, E. Harel, B. E. Koel, and A. A. G. Requicha, "Local detection of electromagnetic energy transport below the diffraction limit in metal nanoparticle plasmon waveguides," *Nature Mater*., vol. 2, pp. 229–232, 2003.

[65] R. de Waele, A. F. Koenderink, and A. Polman, "Tunable nanoscale localization of energy on plasmon particle arrays," *Nano Lett*., vol. 7, pp. 2004–2008, 2007.

[66] R. F. Oulton, V. J. Sorger, T. Zentgraf, R.-M. Ma, C. Gladden, L. Dai, G. Bartal, and X. Zhang, "Plasmon lasers at deep subwavelength scale," *Nature*, vol. 461, pp. 629–632, 2009.

[67] Y.-F. Xiao, B.-B. Li, X. Jiang, X. Hu, Y. Li, and Q. Gong, "High quality factor, small mode volume, ring-type plasmonic microresonator on a silver chip," *J. Phys. B, At. Mol. Opt. Phys*., vol. 43, pp. 035402-1–035402-5, 2010.

[68] B. Wang and G. P. Wang, "Plasmon Bragg reflectors and nanocavities on flat metallic surfaces," *Appl. Phys. Lett*., vol. 87, pp. 013107-1–013107-3, 2005.

[69] N. Yu, Q. J. Wang, M. A. Kats, J. A. Fan, S. P. Khanna, L. Li, A. G. Davis, E. H. Linfield, and F. Capasso, "Designer spoof surface plasmon structures collimate terahertz laser beams," *Nature Mater*., vol. 9, pp. 730–735, 2010.

[70] Y.-F. Xiao, C.-L. Zou, B.-B. Li, Y. Li, C.-H. Dong, Z.-F. Han, and Q. Gong, "High-Q exterior whispering-gallery modes in a metal-coated microresonator," *Phys. Rev. Lett*., vol. 105, pp. 153902-1–153902-4, 2010.

[71] B. Wiley, Y. Sun, and Y. Xia, "Polyolsynthesis of silver nanostructures: control of product morphology with Fe(II) or Fe(III) Species," *Langmuir*, vol. 21, pp. 8077–8080, 2005.

[72] E. D. Palik, *Handbook of Optical Constants of Solids*. New York: Academic, 1997.

[73] N. P. de Leon, "Engineering confined electrons and photons at the nanoscale," Ph.D. dissertation, Harvard University, Cambridge, MA, 2011.

[74] B. D. Busbee, S. O. Obare, and C. J. Murphy, "An improved synthesis of high-aspect ratio gold nanorods," *Adv. Mater*., vol. 15, pp. 414–416, 2003.

[75] K. Vasilev, T. Zhu, M. Wilms, G. Gillies, I. Lieberwirth, S. Mittler, W. Knoll, and M. Kreiter, "Simple, one-step synthesis of gold nanowires in aqueous solution," *Langmuir*, vol. 21, pp. 12399–12403, 2005.

[76] F. Kim, K. Sohn, J. Wu, and J. Huang, "Chemical synthesis of gold nanowires in acidic solutions," *J. Amer. Chem. Soc*., vol. 130, pp. 14442–14443, 2008.

[77] X. Lu, M. S. Yavuz, H.-Y. Tuan, B. A. Korgel, and Y. Xia, "Ultrathin gold nanowires can be obtained by reducing polymeric strands of oleylamine-AuCl complexes formed via aurophilic interaction," *J. Amer. Chem. Soc*., vol. 130, pp. 8900–8901, 2008.

[78] Z. Huo, C.-K. Tsung, W. Huang, X. Zhang, and P. Yang, "Sub-two nanometer single crystal Au nanowires," *Nano Lett*., vol. 8, pp. 2041–2044, 2008.

[79] C. Wang, Y. Hu, C. M. Lieber, and S. Sun, "Ultrathin Au nanowires and their transport properties," *J. Amer. Chem. Soc*., vol. 130, pp. 8902–8903, 2008.

[80] C.-H. Dong, X.-F. Ren, R. Yang, J.-Y. Duan, J.-G. Guan, G.-C. Guo, and G.-P. Guo, "Coupling of light from an optical fiber taper into silver nanowires," *Appl. Phys. Lett*., vol. 95, pp. 221109-1–221109-3, 2009.

[81] A. L. Pyayt, B. Wiley, Y. Xia, A. Chen, and L. Dalton, "Integration of photonic and silver nanowire plasmonic waveguides," *Nature Nanotechnol*., vol. 3, pp. 660–665, 2008.

[82] P. Neutens, P. Van Dorpe, I. De Vlaminck, L. Lagae, and G. Borghs, "Electrical detection of confined gap plasmons in metal-insulator-metal waveguides," *Nature Photon*., vol. 3, pp. 283–286, 2009.

[83] M. W. Knight, H. Sobhani, P. Nordlander, and N. J. Halas, "Photodetection with active optical antennas," *Science*, vol. 332, pp. 702–704, 2011.

[84] E. S. Barnard, R. Pala, and M. L. Brongersma, "Photocurrent mapping of near-field optical antenna resonances," *Nature Nanotechnol*., vol. 6, pp. 588–593, 2011.

[85] R. W. Heeres, S. N. Dorenbos, B. Koene, G. S. Solomon, L. P. Kouwenhoven, and V. Zwiller, "On-chip single plasmon detection," *Nano Lett*., vol. 10, pp. 661–664, 2010.

[86] W. Pernice, C. Schuck, O. Minaeva, M. Li, G. N. Goltsman, A. V. Sergienko, and H. X. Tang, "High speed travelling wave single-photon detectors with near-unity quantum efficiency," 2011.

[87] C. L. Yu, A. L. Falk, N. P. de Leon, C. Colombo, M.-H. Jo, A. FontcubertaI Morral, M. D. Lukin, and H. Park, "Electrically coupled surface plasmon polaritons in nanowire circuits," 2011, to be published.

[88] P. Bharadwaj, A. Bouhelier, and L. Novotny, "Electrical excitation of surface plasmons," *Phys. Rev. Lett*., vol. 106, pp. 226802-1–226802-4, 2011.

[89] R. J. Walters, R. V. A. van Loon, I. Brunets, J. Schmitz, and A. Polman, "A silicon-based electrical source of surface plasmon polaritons," *Nature Mater*., vol. 9, pp. 21–25, 2010.

[90] P. Neutens, L. Lagae, G. Borghs, and P. Van Dorpe, "Electrical excitation of confined surface plasmon polaritons in metallic slot waveguides," *Nano Lett*., vol. 10, pp. 1429–1432, 2010.

[91] D. M. Koller, A. Hohenau, H. Ditlbacher, N. Galler, F. Reil, F. R. Aussenegg, A. Leitner, E. J. W. List, and J. R. Krenn, "Organic plasmon-emitting diode," *Nature Photon*., vol. 2, pp. 684–687, 2008.

[92] A. V. Krasavin and N. I. Zheludev, "Active plasmonics: Controlling signals in Au/Ga waveguide using nanoscale structural transformations," *Appl. Phys. Lett*., vol. 84, pp. 1416–1418, 2003.

[93] T. Nikolajsen, K. Leosson, and S. I. Bozhevolnyi, "Surface plasmon polariton based modulators and switches operating at telecom wavelengths," *Appl. Phys. Lett*., vol. 85, pp. 5833–5835, 2004.

[94] R. A. Pala, K. T. Shimizu, N. A. Melosh, and M. L. Brongersma, "A nonvolatile plasmonic switch employing photochromic molecules," *Nano Lett*., vol. 8, pp. 1506–1510, 2008.

[95] J. A. Dionne, K. Diest, L. A. Sweatlock, and H. A. Atwater, "PlasMOStor: A metal-oxide-Si field effect plasmonic modulator," *Nano Lett*., vol. 9, pp. 897–902, 2009.

[96] D. Pacifici, H. J. Lezec, and H. A. Atwater, "All-optical modulation by plasmonic excitation of CdSe quantum dots," *Nature Photon*., vol. 1, pp. 402–406, 2007.

[97] M. Gather, K. Meerholz, N. Danz, and Leosson, "Net optical gain in a plasmonic waveguide embedded in a fluorescent polymer," *Nature Photon*., vol. 4, pp. 457–461, 2010.

[98] K. F. MacDonald, Z. L. Samson, M. I. Stockman, and N. I. Zheludev, "Ultrafast active plasmonics," *Nature Photon*., vol. 3, pp. 55–58, 2008.

[99] D. J. Bergman and M. I. Stockman, "Surface plasmon amplification by stimulated emission of radiation: Quantum generation of coherent surface plasmons in nanosystems," *Phys. Rev. Lett*., vol. 90, pp. 027402-1–027402-4, 2003.

[100] M. A. Noginov, G. Zhu, A. M. Belgrave, R. Bakker, V. M. Shalaev, E. E. Narimanov, S. Stout, E. Herz, T. Suteewong, and U. Wiesner,

"Demonstration of a SPASER-based nanolaser," *Nature*, vol. 460, pp. 1110–1112, 2009.
[101] R.-M. Ma, R. F. Oulton, V. J. Sorger, G. Bartal, and X. Zhang, "Room-temperature sub-diffraction-limited plasmon laser by total internal reflection," *Nature Mater.*, vol. 10, pp. 110–113, 2010.
[102] G. Bjork and Y. Yamamoto, "Analysis of semiconductor microcavity lasers using rate equations," *IEEE J. Quantum Electron.*, vol. 27, no. 11, pp. 2386–2396, Nov. 1991.
[103] I. Fushman, D. Englund, and J. Vuckovic, "Coupling of PbS quantum dots to photonic crystal cavities at room temperature," *Appl. Phys. Lett.*, vol. 87, pp. 241102-1–241102-3, 2005.
[104] M. Nomura, S. Iwamoto, K. Watanabe, N. Kumagai, Y. Nakata, S. Ishida, and Y. Arakawa, "Room temperature continuous-wave lasing in photonic crystal nanocavity," *Opt. Exp.*, vol. 14, pp. 6308–6315, 2006.
[105] M. D. Lukin, "Trapping and manipulating photon states in atomic ensembles," *Rev. Mod. Phys.*, vol. 75, pp. 457–472, 2003.
[106] S. E. Harris and Y. Yamamoto, "Photon switching by quantum interference," *Phys. Rev. Lett.*, vol. 81, pp. 3611–3614, 1998.
[107] M. Fleischhauer, A. Imamoglu, and J. P. Marangos, "Electromagnetically induced transparency: Optics in coherent media," *Rev. Mod. Phys.*, vol. 77, pp. 633–673, 2005.
[108] K. M. Birnbaum, A. Boca, R. Miller, A. D. Boozer, T. E. Northup, and H. J. Kimble, "Photon blockade in an optical cavity with one trapped atom," *Nature*, vol. 436, pp. 87–90, 2005.
[109] B. Dayan, A. S. Parkins, T. Aoki, E. P. Ostby, K. J. Vahala, and H. J. Kimble, "A photon turnstile dynamically regulated by one atom," *Science*, vol. 319, pp. 1062–1065, 2008.
[110] R. Miller, T. E. Northup, K. M. Birnbaum, A. Boca, A. D. Boozer, and H. J. Kimble, "Trapped atoms in cavity QED: coupling quantized light and matter," *J. Phys. B, At. Mol. Opt. Phys*, vol. 38, pp. S551–S565, 2005.
[111] D. E. Chang, A. S. Sorensen, E. A. Demler, and M. D. Lukin, "A single-photon transistor using nanoscale surface plasmons," *Nature Phys.*, vol. 3, pp. 807–812, 2007.
[112] C. Monroe and M. D. Lukin, "Remapping the quantum frontier," in *Physics World*, 2008, pp. 32–39.
[113] Q. A. Turchette, D. Kielpinski, B. E. King, D. Leibfried, D. M. Meekhof, C. J. Myatt, M. A. Rowe, C. A. Sackett, C. S. Wood, W. M. Itano, C. Monroe, and D. J. Wineland, "Heating of trapped ions from the quantum ground state," *Phys. Rev. A*, vol. 61, pp. 063418-1–063418-8, 2000.
[114] C. Stehle, H. Bender, C. Zimmermann, D. Kern, M. Fleischer, and S. Slama, "Plasmonically tailored micropotentials for ultracold atoms," *Nature Photon.*, vol. 5, pp. 494–498, 2011.

Nathalie P. de Leon was born in Makati, Philippines, in 1982. She received the B.S. degree in chemistry from Stanford University, Palo Alto, CA, in 2004, and the Ph.D. degree in chemical physics from Harvard University, Cambridge, MA, in 2011.

She is currently an Element Six Postdoctoral Fellow in the Departments of Physics and of Chemistry and Chemical Biology, Harvard University, working in the labs of M. Lukin and H. Park.

Mikhail D. Lukin was born in Moscow, Russia, in 1971. He received the Diploma degree in applied physics from the Moscow Institute of Physics and Technology, Moscow, in 1993, and the Ph.D. degree in physics from Texas A&M University, College Station, in 1998.

He is currently a Professor in the Department of Physics, Harvard University, Cambridge, MA.

Hongkun Park was born in Seoul, Korea, in 1967. He received the B.S. degree in chemistry from Seoul National University, Seoul, in 1990, and the Ph.D. degree in physical chemistry from Stanford University, Palo Alto, CA, in 1996.

He is currently a Professor in the Departments of physics and of Chemistry and Chemical Biology, Harvard University, Cambridge, MA.